Geotechnical Engineering Journal of the SEAGS & AGSSEA Vol. 45 No.3 September 2014 ISSN 0046-5828

Performance of Rail Embankments Constructed with Coal Ash as a Structural Fill Material: Centrifuge Study

B.V.S. Viswanadham[1] and V.K. Mathur[2]
[1]*Professor, Department of Civil Engineering, Indian Institute of Technology Bombay, Powai, Mumbai – 400 076, India*
[2]*General Manager, Environment, Ash Management, NTPC Limited, A-11, NFL Premises, Sector-24, Noida -201301, India*
Email: viswam@civil.iitb.ac.in

ABSTRACT: The objective of the present study is to understand the stability and deformation behavior of rail embankments constructed with coal ash as a structural fill material through centrifuge model tests. Two types of railway embankments were modeled: 1) Clay confined coal ash embankment with 1V:2H slope of 11 m height and 2) Geogrid reinforced coal ash embankment with 2V:1H slope of 4 m height using a large beam centrifuge facility available at IIT Bombay. Considering the nature of railway embankments and possibility of building-up of ground water table due to rainfall, a seepage tank simulator was used to induce seepage into the rail embankment during centrifuge tests. After establishing steady-state seepage conditions, the crest of the embankment was subjected to an incremental static loading pressure distributed through a rigid strip footing up to 700 kPa or failure, whichever occurred first. Additionally, an option of provision of drainage at the mid-height of the railway embankment was also explored for clay-confined coal ash embankments. Based on the analysis and interpretation of centrifuge model test results, for a soil confined coal ash embankment with 1V:2H slope with a confinement layer of 1.5 m thickness in the top-half height and berms in the bottom-half zone was observed to sustain an ultimate load bearing pressure of 400 kPa. Geogrid reinforcement layers in a reinforced coal ash embankment with 2V:1H slope were observed to experience straining after applying a bearing pressure of 250 kPa in the top-half zone and indicating a need to provide high strength layers in top-half zone. Further, results of stability analysis of soil confined coal ash embankment models constructed with coal ash as a fill material were found to corroborate well with physically observed centrifuge test results.

1. INTRODUCTION

Coal ash is the by-product of coal based thermal power plants and its disposal is a major problem from an environmental point of view in many countries and also requires a lot of disposal areas. Coal ash is referred for ash accumulated in the ash pond dam sites. It is estimated that by the year 2012 coal ash generation in India will be reaching nearly 160 million tones. Coal ash has been successfully used as a structural fill material for constructing highway embankments in number of locations throughout the world. However, studies pertaining to the usage of coal ash as a structural fill material for constructing railway embankments are very much limited.

Many investigators like [Gray and Lin (1972); Digioia Jr. and Nuzzo (1972); Leonards and Balley (1982); Toth et al. (1988),;Martin et al. (1991); Das et al. 2009] have analyzed coal ash generating from different power plants all over the world for different applications such as, compacted coal ash embankments, sub-base in road construction, filling low-lying areas, etc. The main emphasis is to identify suitable methodology for bulk consumption of the material like coal ash generated from the coal based thermal powers stations located all over the world. To minimize the potential for environmental problems with structural coal ash embankments, it is logical to use only coal ash that has been shown to have safe leaching characteristics and also to restrict the rate of water permeability of fills. This was envisaged through capillary cut-offs at the bottom of embankment and provision of confinement layer along side slopes. The major concerns with respect to the potential impact of a coal ash embankment on the local environment are wind erosion, surface-water erosion, dissolution in surface runoff and dissolution in rainfall percolating to ground water. To counter some of the above-mentioned factors, the coal ash is encapsulated with a relatively low permeable soil cover. The low-permeable soil cover generally consists of clayey silt or silty clay type soils. The soil cover impedes or controls dissolution of coal ash due to surface run-off and also acts as a confinement layer. With this sort of coal ash confining system, it is possible to retain strength properties of coal ash. According to Lewis (1976); Faber and DiGioia Jr. (1976); Toth et al. (1988); Martin et al. (1990), on an average a slope of 1V: 2H (26.5° with the horizontal surface) was adopted for constructing highway embankments with a confinement layer ranging from 450 mm to 2000 mm thickness is provided all around to prevent erosion and contain coal ash safely. It is also in practice to provide thin horizontal barriers made of impermeable soil to contain the coal ash in cells.

As these soil confined coal ash embankments are constructed on a soil having adequate bearing capacity, the following five modes of failures are envisaged. They are: 1) Failure of cover due to raising water pressure in coal ash, 2) Global failure surface extending from the edge of the loaded area, 3) Punching of loaded area in blanket layer causing differential movements at loading edges, and 4) Sliding movement of blanket portion above embankment level. Failure of cover soil can occur due to inadequate cover thickness. This can also occur due to seasonal drying and wetting of soil cover leading to cracking or opening of soil cover. Opening of soil cover supports eroding tendency of coal ash out of the bund. This can result in differential sinking of rail tracks with time. Figures 1-2 depict a typical observed feature in the field wherein soil confined coal ash embankment was constructed (NTPC report, 2008).

As can be noted from the above cited literature, coal ash has been used as a structural fill material in majority of approach roads/highway embankments. Literature pertaining to the utilization of coal ash as a structural fill material for railway embankment construction is very much limited. Sunaga and Sekine (1992) reported about utilization of potential of coal ash as a structural material for railway embankments/construction of raised intersections for rail metro in Japan. Apart from these, details pertaining to the behavior and application are very much scattered. Hence, this forms the relevance and current interest of the present study. In addition, to the best of authors knowledge, attempts towards understanding the response of rail embankments constructed with coal ash as a structural fill through centrifuge based small-scale physical modeling are limited. The main drawback of the reduced scale physical modeling at normal gravity is that stress levels are much smaller than that of the prototype. As the behavior of soils is mainly governed by confining stresses, the reduced scale models may not represent the true behavior. Identical stress field in both model and prototype can be achieved by adopting centrifuge modeling technique. In a centrifuge, the behavior of prototype structures can be studied as scaled-down models in a controlled environment, while preserving the stress states required developing appropriate soil properties. Therefore, centrifuge testing is an appropriate tool for studying the behavior of embankments constructed with coal ash as a structural fill material.

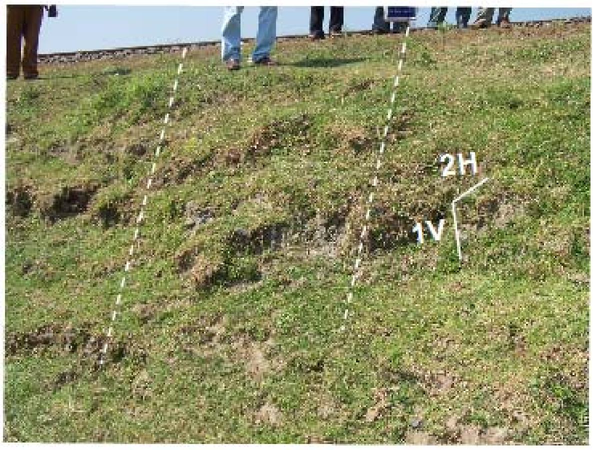

Figure 1- Status of a slope of Tamluk Digha railway embankment (South Eastern Railway, India) constructed with coal ash as a structural fill (NTPC report, 2008)

Figure 2 Close view of the slope along Tamluk Digha railway embankment (NTPC report, 2008)

In this paper, centrifuge test results of two soil confined coal ash embankments of 11 m height were compared. In addition, centrifuge test results of a 4 m high 2V:1H slope geogrid reinforced slope were discussed. Considering the nature of railway embankments and possibility of building-up of ground water table due to rainfall, a seepage tank simulator was used to induce seepage. After establishing steady-state seepage conditions, the crest of the embankment was subjected to an incremental static loading pressure distributed through a rigid strip footing up to 700 kPa or failure, whichever occurred first. Additionally, significance of confining layer and an option of provision of drain vent at the mid-height of a clay-confined coal ash embankment was also explored.

2. EXPERIMENTAL STUDIES IN A CENTRIFUGE

The 4.5m radius large beam centrifuge facility available at Indian Institute of Technology Bombay was used for model tests presented in this paper. The centrifuge capacity is 2500 g-kN with a maximum payload of 25 kN at 100g and at higher acceleration of 200g the allowable payload is 6.25 kN. Specifications in detail are discussed by Chandrasekaran (2001) and Viswanadham et al. (2009). Figure 3 depicts a large beam centrifuge facility used in the present study.

Figure 3 View of a 4.5 m radius large beam centrifuge facility at IIT Bombay

2.1 Scaling Considerations

Conventionally, it is assumed that the soil in the centrifuge model and prototype are identical. In a centrifuge, stress similarity is achieved by accelerating a model of scale 1/N to N times the earth's gravity (N = Scale factor or g-level). Scaling considerations and errors due to centrifuge modeling are discussed in detail by Schofield (1980). The soil particles in a centrifuge model can not be scaled down to scale the soil particles of prototype, while other model dimensions can be modeled down and this effect is called as grain size effect. However, with respect to centrifuge model tests on rail embankments with coal ash as a structural fill, this aspect is satisfied because of similarity of grain size distribution of coal ash in the model and in the field. In the present study, scale factors for seepage velocity $(v_s)_m$ = N$(v_s)_p$, seepage time $t_m = t_p/N^2$ and pore water pressure $u_m = u_p$ were used (where suffix m = centrifuge model; p = prototype).

2.2 Model Materials

2.2.1 Coal ash and Local soil

Coal ash was collected from Kahalgaon Super thermal power plant in Bihar state of India. The grain size distribution of the coal ash showed that it contains 64% sand, and 36% silt size particles. It is classified as an ASTM class F coal ash with a calcium content of 1.94% (Sridharan et al. 2000). The effective particle size d_{10} is 0.02 mm and is classified as SM according to Unified Soil Classification system. The maximum dry unit weight $\gamma_{d,max}$ and optimum moisture content OMC of the coal ash are 13.2 kN/m^3 and 22% (standard Proctor compaction). Saturated direct shear box tests on coal ash moist-compacted at its $\gamma_{d,max}$ and OMC gave an internal friction angle ϕ of 34° and cohesion as zero. The coefficient of permeability k of coal ash moist-compacted at $\gamma_{d,max}$ and OMC is 2.58 x 10^{-6} m/s. In order to construct base soil, side cover and top cover soil, locally available soil at Kahalgaon Super thermal plant site was used. The grain size distribution of the Kahalgaon soil contains 20% sand, 57% silt, and 23% clay size particles. Liquid limit and plasticity index are 46% and 26% respectively. It is classified as CL according to Unified Soil classification system. The maximum dry unit weight $\gamma_{d,max}$ and optimum moisture content OMC of the local soil are 17.4 kN/m^3 and 16% (standard Proctor compaction). The cohesion and angle of internal friction ϕ of the local soil moist-compacted at $\gamma_{d,max}$ and OMC are 50 kN/m^2 and 16° (Direct shear box test). The coefficient of permeability k of local soil moist-compacted at $\gamma_{d,max}$ and OMC is 2.5 x 10^{-8} m/s.

2.2.2 Geogrid

A major difficulty encountered in model studies involving geogrid materials is selection, modelling and instrumentation of ideal materials. Contrary to soils, the similitude condition does not allow the use of identical materials in model and prototype studies. The reinforcement elements are mainly planar layers like uniaxial geogrids in the case of slopes and walls or biaxial geogrids for embankments on soft ground, pavements on weak subgrade, and landfill liners. One alternative is to study the response of these structures by constructing full-scale structures in the field with extensive instrumentation. However, costs associated with prototype instrumentation may also be significant and the reliability of the collected data was often questionable. Among the different categories of reinforced soil structures, lack of field data is particularly striking for the case of geosynthetic reinforced slopes, which may result in significantly high factors of safety have been incorporated into current design methodologies. In such situations, application of the centrifuge modelling technique for studying the deformation behaviour of geosynthetic reinforced slopes is a viable option and moreover soil-geosynthetic interaction is highly influenced by the presence of prototype stress conditions.

At least ten to fifteen varieties of synthetic (many having different styles) geogrids are available. They differ considerably in geometry and mechanical properties. The manufacturers attempt to vary the typical geometrical characteristics and tensile load characteristics (as manufacturing process variable) in order to achieve a desired geogrid. As tensile load characteristic of synthetic material is mainly dependent on the composition and type of raw material, it has become one of the manufacturing process variables. The properties of these geogrids are specified based on: (i) rib cross-sectional area, (ii) grid opening size, (iii) tensile strength, and (iv) type of material composition. The criterion for scaling down the reinforcement function of the geocomposite in centrifuge based small scale physical modeling is based on: (i) tensile load-strain behavior and (ii) frictional bond behavior along soil-geogrid interface. Scaling considerations given by Viswanadham and König (2004); and Rajesh and Viswanadham (2012) were used to achieve the modeling geogrids. The frictional bond behavior along soil-geogrid interface was assumed to be achieved by ensuring identical percentage open area *f* between model and prototype geogrids. The percentage open area *f* expressed in percentage is the ratio of area formed by grid opening sizes to area formed by grid opening sizes measured up to center of width of ribs. The expression for percentage open area can be written as $f = a_l a_t/[(a_l + b_l)(a_t + b_t)]$ (where, a_l and a_t are grid opening sizes in longitudinal and transverse directions and b_l and b_t the widths of the rib in longitudinal and transverse directions respectively), of the geogrid. Table 1 summarizes general scaling relations relevant to centrifuge modelling.

3. MODEL TEST PACKAGE, TEST PROGRAMME AND TEST PROCEDURE FOR CLAY CONFINED COAL ASH EMBANKMENTS

The container used to build the models for this study was a strongbox having dimensions inside of 760 mm long, 200 mm wide, and 410 mm deep. All walls of the box except for the front are composed of steel plates. A cross-section of the model test package is presented in Figure 4. Considering symmetry, only right half section of bund was selected. The front wall is a viewing window, consisting of a thick Perspex glass sheet. To reduce any boundary effects caused by friction between the coal ash and container walls and to maintain plane-strain conditions, a thin layer of petroleum grease was applied to the container walls, followed by thin polythene sheet strips. This method was adopted by Viswanadham et al. (2009) to reduce friction effects and allow for plane-strain conditions to exist. A seepage tank was custom designed and calibrated to induce seepage in the model slopes. The seepage tank was made of 10mm thick aluminum plates. The internal dimensions of the seepage tank were 80mm x 360mm x 200mm. One wall of the seepage tank was perforated to allow seepage of water. The perforated wall of the seepage tank was covered with a layer of non-woven geotextile to prevent clogging of the perforations by the soil/coal ash particles. Table 2 shows the details of centrifuge model tests discussed in this paper. Two slope models REM11 and REM12 having 11 m height were presented. Dimensions of different components of rail embankment models constructed with coal ash core confined with a local soil and blanket layer are marked in Fig. 4 and given in model and prototype dimensions.

Table 1 Scaling relationships for modelling geogrid

Parameter	**Units**	**Centrifuge model/prototype**
a_l, a_t, b_l, b_t, t*	m	1/N
Cross-sectional area of rib/unit length A′	m	1/N
Percentage Open area *f*	[%]	1
Tensile load T_g	[kN/m]	1/N
Strain ε_g	[%]	1
Secant modulus J_g	[kN/m]	1/N
Bond stress τ_b	[kN/m^2]	1

*a_l, a_t = grid opening sizes in longitudinal and transverse directions; b_l, b_t = width of ribs in longitudinal and transverse directions; *t* = average thickness of the rib.

Slope models were *H* (m) in height which excludes a blanket layer thickness of t_b (m) and a base soil thickness of *D* (m). The slopes were constructed with a slope inclination of 26º (1V:2H). Drainage was provided at the downstream end by providing a drain at the right end of the container. After compacting base soil layer, a thin layer of sand of about 6 mm (~0.3 m) was placed in both the models. To prevent erosion of soil particles, a thin non-woven geotextile fabric was provided by wrapping back into the slope. In all models, thickness of top soil cover is provided as t_t mm and side cover thickness of t_c mm. In model REM11, the cover soil thickness above the second berm is 1 m and in model REM12 it is 1.5 m. In addition, model REM12 has also a provision of drain at mid-height (i.e. second berm from the toe). The models were instrumented using three Linearly Variable Differential Transformers (LVDTs) on the top surface of the slope to measure the displacements and out of these, one was placed on the loading plate. Five Pore water Pressure Transducers (PPTs) were used to measure the pore water pressure during the progress of the test.

Table 2 Details of centrifuge tests

Test legend	**N**	**H (m)**	**D (m)**	**t_c (m)**	**t_t (m)**	**t_b (m)**	**Mid-height drainage**
REM11	50	0.22 (11)	0.074 (3.7)	0.02 (1)	0.012 (0.6)	0.006 (0.3)	No
REM12	54	0.204 (11)	0.090 (4.8)	0.027 (1.5)	0.012 (0.64)	0.006 (0.32)	Yes

t_c = thickness of side soil cover in the upper portion of the slope; Dimensions for H and t_c are given in corresponding prototype dimensions within the parentheses; Side berms were cut to shape from the initially compacted thick soil cover.

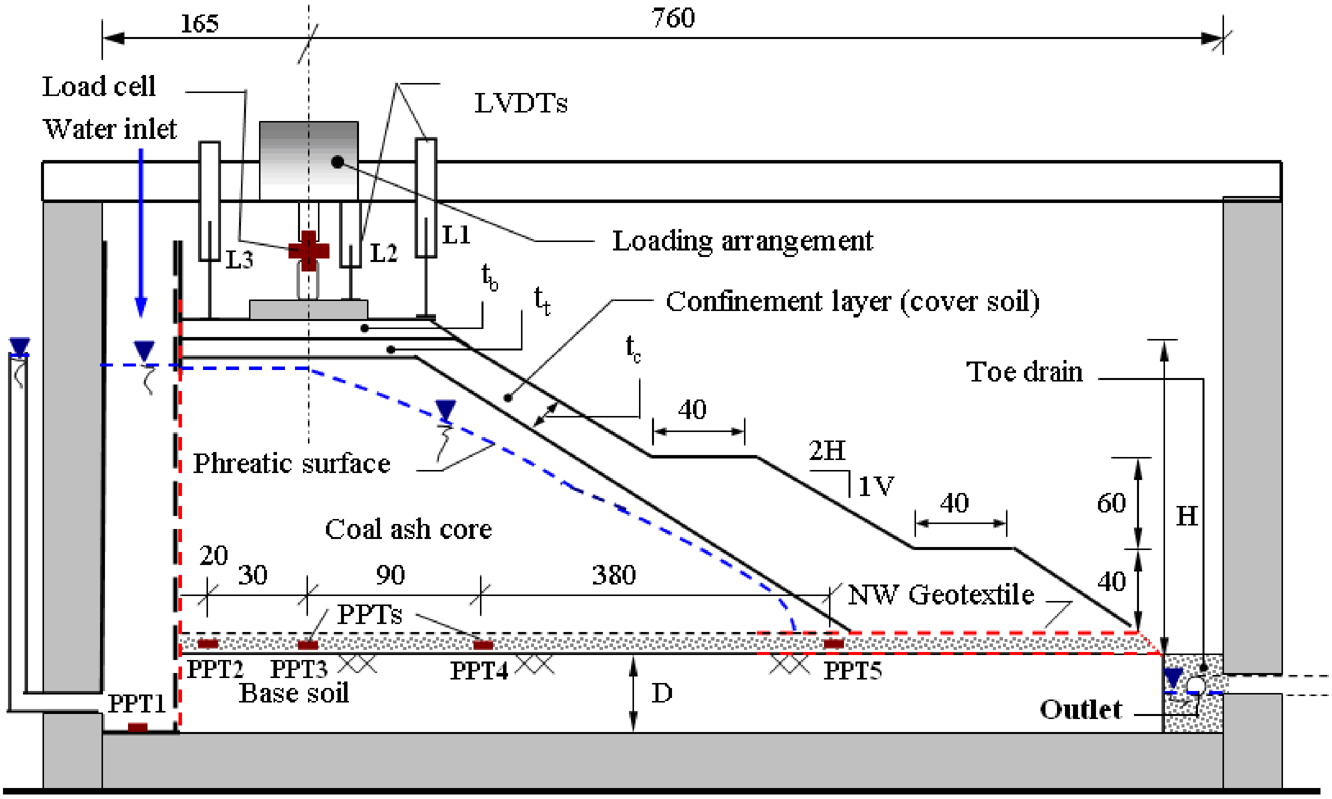

Figure 4 Cross-section of a model test package (all dimensions are in mm)

After the compaction of base layer was completed, temporary wooden supports were placed to achieve the desired slope inclination. This support has got a special provision to compact the side cover parallel to the slope surface with the local soil. The slope was constructed in layers. After completion of each layer, specially designed L-shaped plastic markers made of thin transparency sheets were placed to study the movement of coal ash and soil cover during the test. To allow free movement of the markers, white petroleum grease was applied on the sides of the markers in contact with the container and the soil. Colored food dye was placed at intervals on the top of each layer to visualize the movement of water during seepage. After construction of the slope, the entire slope along with top, side cover soil and blanket layer was allowed to inundate in water for about 24 hours at normal gravity in the laboratory. After saturation, a rigid stainless steel strip footing of 50 mm thick was placed with its center 165 mm from the inside left edge of seepage tank, and connected to a loading cell (Figure 5). The crest of the slope was located 140mm from the left edge of seepage tank, so the load was applied at a setback distance d = 70 mm from the slope crest. After the ramping time, the centrifuge was allowed to rotate at a constant revolutions per minute (rpm) corresponding to a desired g-level, given in Table 2. After attaining a desired g-level, water was allowed to seep in through the coal ash core and its behavior was observed for global failure or localized failures, if any. After establishing steady state seepage conditions, with the help of pneumatic cylinder connected to the footing via a load cell, a static pressure was applied incrementally. Each increment of static pressure was maintained only for a short duration of 5 minutes in model dimensions and increased up to 700 kPa or failure, whichever occurred first. The proceedings of the test were grabbed through a Canon make digital photo camera mounted along with the model to view the front elevation of the model. The data from the LVDTs and PPTs was obtained using the on-board data acquisition system.

Figure 5 shows the loading arrangement for inducing load at the top surface of the embankment along with the load cell.

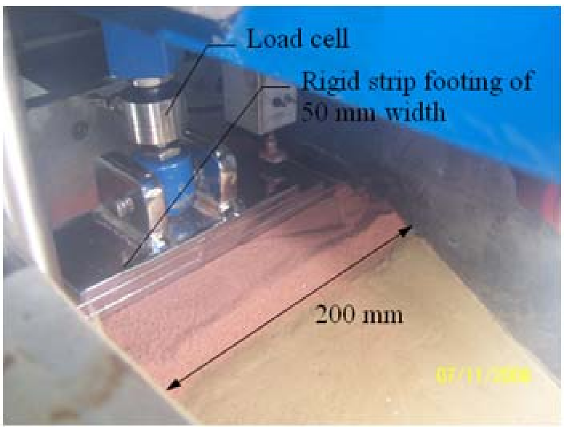

Figure 5 Loading arangement for inducing load at the top surface of the embankment

3.1 Analysis and interpretation of centrifuge test results

Figure 6 gives variation of measured pore-water pressure with time in prototype dimensions for model REM11. Within 2 to 3 days of seepage time, steady state seepage conditions were found to be established. This was maintained to simulate raise of ground water table within the coal ash core due to rainfall water infiltration into rail embankment. During this stage, model was monitored for any global failure or localized failures within the soil cover of the soil confined coal ash embankment. Figures 7a-7b show measured variation of settlements with seepage time (from L1, L2, L3, as shown in Figure 4) of the slope along with footing plate. In the case of model REM11, beyond 7.5 days of seepage time a steady increase in the footing plate was observed. Photographs captured during the various stages of seepage through model REM11 indicate side cover failure, as shown in Figures 8a-8b. Results of these tests are discussed in brief by Viswanadham et al (2012).

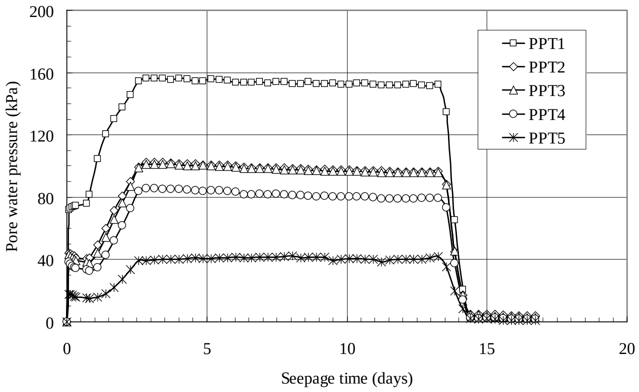

Figure 6 Variation of pore water pressure with seepage time for model REM11

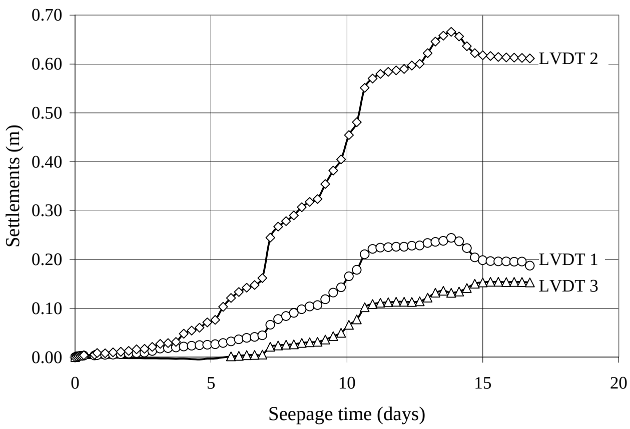

a) Model REM11

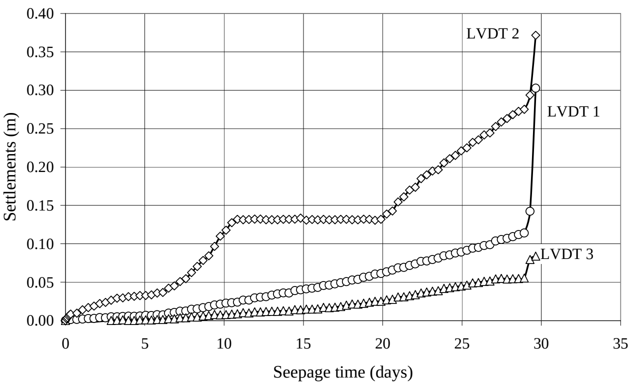

b) Model REM12

Figure 7 Variation of settlements with time measured for soil confined coal ash embankments (in prototype dimensions)

As can be seen from Figure 8, through the failed side cover, exposure of coal ash core can be noted. This necessitates a need for enhancing the t_c from 1 m to 1.5 m and also to check the effect of provision of drain at mid-height. As mentioned in Table 2, the performance of a rail embankment constructed with coal ash as a structural fill material was addressed in model REM12. Figure 9 presents variation of applied pressure with footing settlement for models REM11 and REM12. As can be noted, in the case of model REM11, which was provided with t_c = 1.0 m and without any provision for drainage at mid-height was found experience a footing settlement of 0.5 m at an applied pressure of 200 kPa. This was attributed to the observed behavior depicted in Figure 8. In comparison, for model REM12, at an applied pressure of 200 kPa a footing settlement of only 0.125 m was observed (Figure 9). Further increase in applied pressure beyond 400 kPa, the footing settlement was observed to increase to 0.25 m.

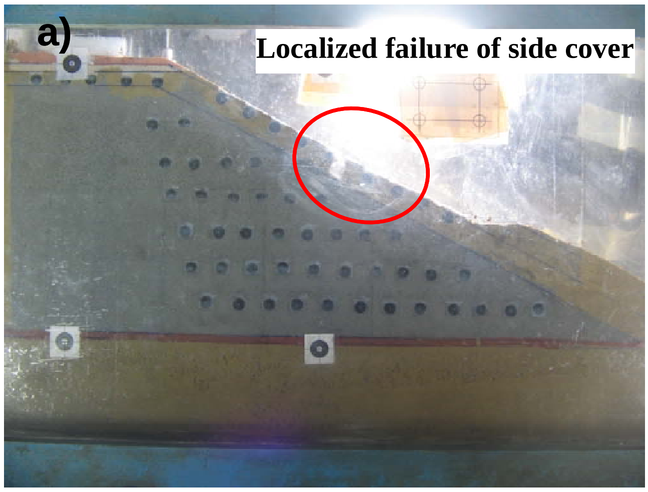

Figure 8 Localized failure of side soil cover for model REM11

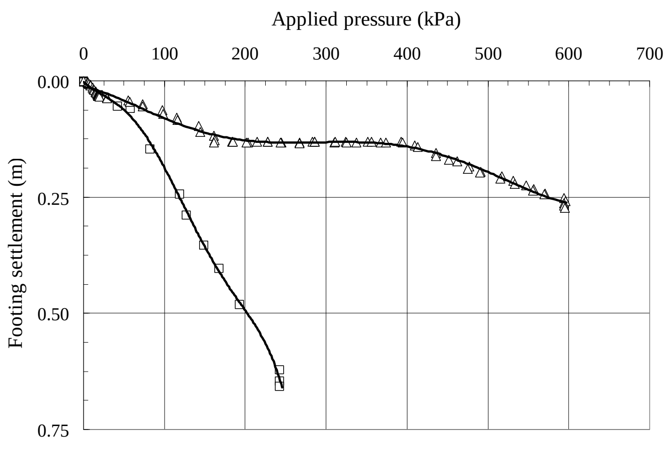

Figure 9 Variation of applied pressure with footing settlement

3.1.1 Applied pressure-footing settlement variation and phreatic surfaces

This applied pressure-footing settlement behavior implies that the model REM12 is superior in performance than the model REM11 and also bring-out the significance of adequate confinement of the side cover above berms and a need for drain provision at mid-height.

Figure 10 shows variation of head of water with the horizontal distance from the left edge of the seepage tank for models REM11 and REM12. These phreatic surfaces were plotted during penultimate stages of the centrifuge test and were obtained by converting the measured pore-water pressure at a specified stage of the seepage. As can be noted from Figure 10, the presence of mid-height drain helps to drain the water rapidly and lead to a depletion of phreatic surface. However, a toe pressure of 40 kPa was observed to develop in both the models.

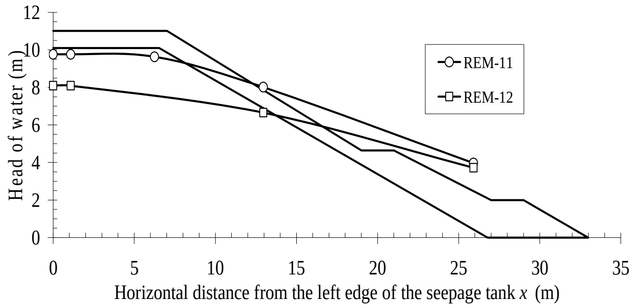

Figure 10 Plot showing efficacy of drain at the level of second berm from toe

3.1.2 Stability analysis of model REM12

In the present study, slope stability analysis was performed using SLOPE/W software (Geostudio, 2007). Analysis was carried-out for a phreatic surface exhibiting highest PWP within the bund and with an increase in the applied footing pressure. Variation of factor of safety with applied pressure is plotted in Figure 11 for model REM12. With an increase in the applied footing pressure, a decrease in the factor of safety was observed. At the onset of failure, at a particular magnitude of applied footing pressure, the factor of safety was observed to drop below 1. This implies that at that pressure the section is exhibiting limiting value of applied footing pressure on the bund section. As can be noted from Figure 11, after application of a footing pressure of the magnitude of 400 kPa, the factor of safety of the embankment is 1. This is also found to be in agreement with the measured applied pressure-footing settlement variation (Figure 9). This implies that the equivalent ultimate static pressure of 400 kPa can be applied on rail embankments constructed with coal ash core. Figure 12 show the status of model REM12 at the end of the centrifuge test.

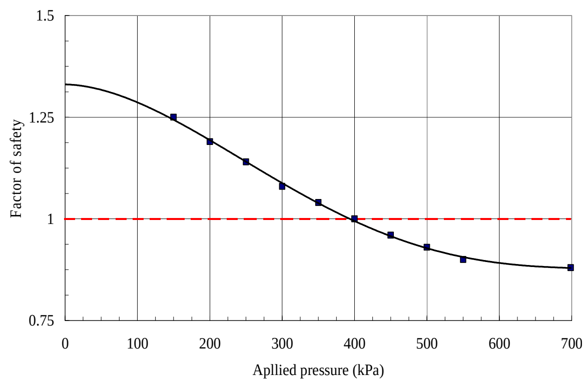

Figure 11 Variation of factor of safety with applied pressure for model REM12

Figure 12 View of model REM12 at the end of centrifuge test

4. MODEL TEST PACKAGE FOR GEOGRID REINFORCED COAL ASH EMBANKMENT

In the present study, a geogrid reinforced steep slope having 2V:1H with a flexible facing was modeled. Flexible facing was adopted using a wrap-around technique. Considering 4 m height and availability of model geogrids, it was decided to model reinforced coal ash embankments at a g-level of 20. Based on scaling considerations presented in Section 2.2.2, a model geogrid G1 was selected. Model geogrid G1 was tested for its wide width tensile strength, as per ASTM D: 4595 (1995). At 5 % strain, value of tensile strength in the longitudinal direction is 0.287 kN/m respectively. The secant stiffness (up to 5 % strain) is 5.74 kN/m in the longitudinal direction. In order to consider confining effect of geogrid, geogrid tensile load obtained from zero-grip tensile tests was adopted, and this corresponds to 0.56 kN/m in model dimensions for model geogrid G1.

The container used for constructing geogrid reinforced coal ash embankments is identical to the one used for clay confined coal ash embankments. A cross-section of the model test package is presented in Figure 13. All slope models were H (mm) in height which excludes a blanket layer thickness of t_b mm and a base soil height of D mm. The slopes were constructed with a slope inclination of 63.4º (2V:1H). After compacting base soil height, first reinforcement layer was placed along with a form work for getting a desired slope inclination. In order to trace movements of geogrid layer, at the onset of seepage and loading, discrete markers were embedded onto geogrid at 20 mm c/c. Movements of markers during various stages of tests were traced to get displacement vectors and strain distribution in reinforcement layers.

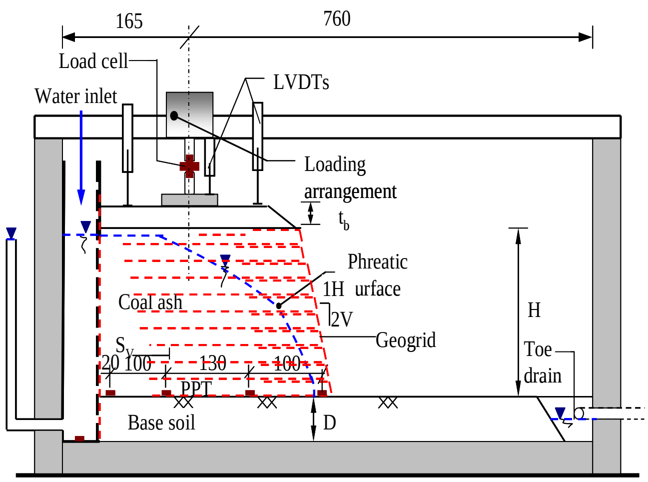

Figure 13 Cross-section of geogrid reinforced coal ash embankment for model REM14 (all dimensions are in mm)

The models were instrumented using three Linearly Variable Differential Transformers (LVDTs) on the top surface of the slope to measure the displacements and out of these, one was placed on the loading plate. Five Pore water Pressure Transducers (PPTs) were used to measure the pore water pressure during the progress of the test. One of them was placed at the bottom of the water tank and the other four were placed in the bottom coal ash layer (as shown in Figure 13). The position of the LVDTs and pore water pressure transducers were also shown.

A rectangular grid of permanent markers was pasted firmly on the inner side of the Perspex sheet. The rectangular grid was 340 mm x 220 mm in size. The model was constructed in layers of 20 mm thickness using moist compacted coal-ash at its maximum dry unit weight and optimum moisture content. After completion of each layer, specially designed L-shaped plastic markers made of thin transparency sheets were placed to study the movement of geogrid layer during the test. To allow free movement of the markers, white petroleum grease was applied on the sides of the markers in contact with the container and soil. Coloured food dye was placed at intervals on the top of each layer to visualize the movement of water during seepage.

After saturation, a rigid strip footing of 50 mm thick was placed with its center 165 mm from the inside left edge of water tank, and connected to a loading cell for all the tests reported in this report. The crest of the slope was located 140mm from the left edge of water tank, so the load was applied at a setback distance x = 70 mm from the slope crest. For all the models, a crest width of 140 mm was maintained throughout the study. The loading arrangement for inducing load at the top surface of the embankment is shown in Figure 5. With this arrangement, end effects due to loading plate can be minimized to a great extent (Sommers and Viswanadham, 2009).

The pore water pressures developed in the slope was measured using pore water pressure transducers placed in the water tank as well as in the base layer of the slopes. From these pore water pressures, the phreatic lines were obtained for all the slopes. Figure 14 gives variation of measure pore-water pressure with time in prototype dimensions and development of phreatic lines within the slope for model REM14. As can be noted from Figure 15, highest value of measured PWP is that of a PPT placed within the water tank. Constant variation of PWP with time indicates the excellent establishment of steady state seepage conditions. In all the experiments, these types of conditions are established by facilitating a flow from left hand side to right hand side of the model. After establishing steady-state seepage conditions, load on the piston of the pneumatic cylinder increased in increments up to a maximum value or to a pressure, where considerable surface settlements are registered catastrophically

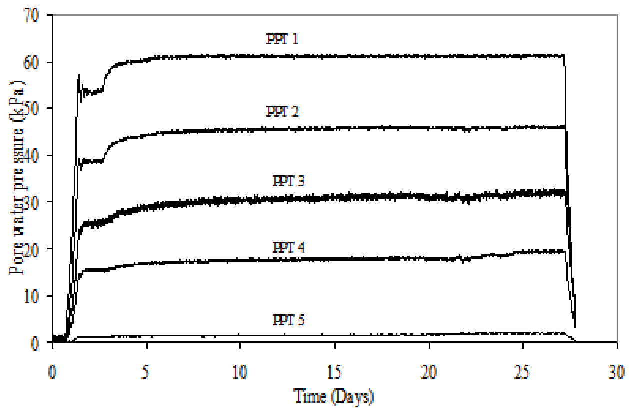

Figure 14 Variation of measured PWP with time for model REM14

Figures 16a-c show the front elevation of model geogrid reinforced coal ash slope at 20g for model REM14. As can be noted from Figure 16c, at the onset of piston pressure p = 400 kPa, formation of crack at the left hand side of the strip footing can be noted. Figure 16c shows development of a failure surface extending up to toe of the slope.

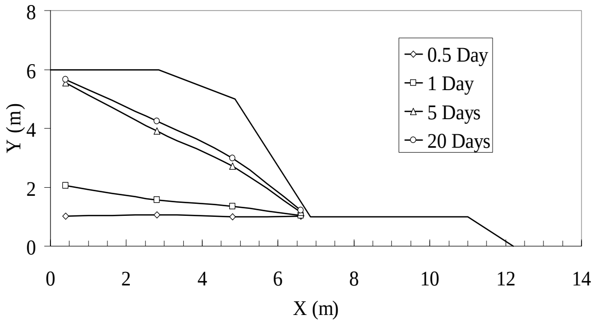

Figure 15 Measured phreatic surfaces for model REM14

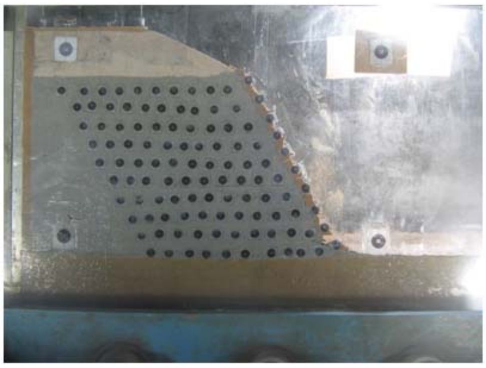

a) Model REM14 20g (p = 10 kPa)

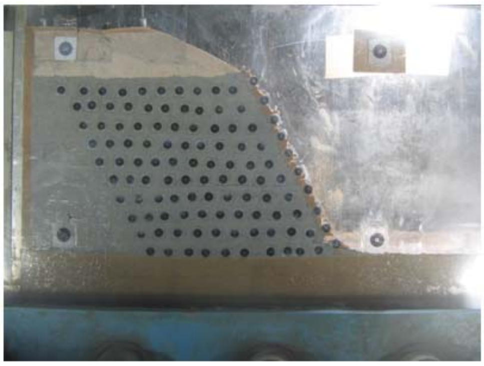

b) Model REM14 20g (p = 350 kPa)

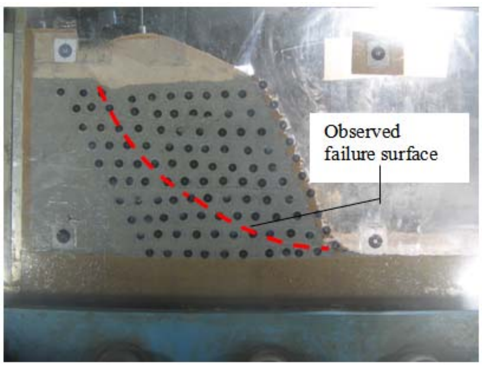

c) Model REM14 20g (p = 450 kPa)

Figure 16 Front elevation of model REM14 during centrifuge test at 20g

Plot showing displacement markers from beginning to end of the centrifuge test at 20g are shown in Figure 17. Pattern of movement of markers indicate a clear and distinct formation of failure surface. Moreover, post-test investigations reveal, that 4 out five reinforcement layers in the top-half of the slope height were found to be ruptured completely. This implies that the mobilization of tensile strength is more than the available tensile strength of the geogrid reinforcement inclusions.

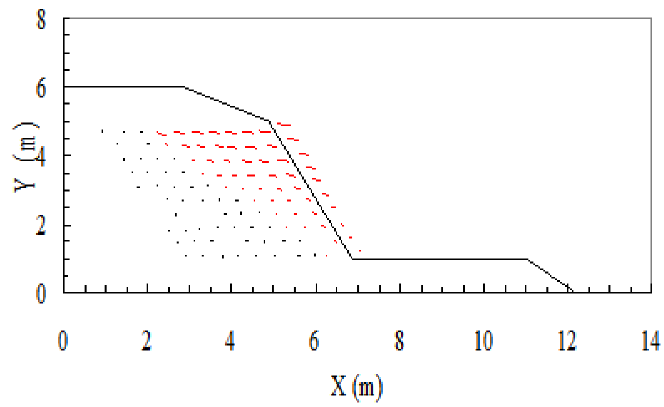

Figure 17 Plot showing displacement vectors from beginning to end of the test (for model REM14)

In the present study, slope stability analysis was performed using SLOPE/W software (Geostudio, 2007). Analysis was carried-out for a phreatic surface exhibiting highest PWP within the bund and with an increase in the applied footing pressure. Variation of FOS with applied footing pressure is plotted for number of cross-sections tested in this study. With an increase in the applied footing pressure, a decrease in the factor of safety was observed. At the onset of failure, at a particular magnitude of applied footing pressure, the factor of safety was observed to drop below 1. This implies that at that pressure the section is exhibiting limiting value of applied footing pressure on the bund section.

For convenience, all intermediate layers were not considered in the analysis. Based on the observations made in model test REM14, innumerable numbers of failure surfaces within the reinforced zone were tried and the failure surface which gave a least value of factor of safety was considered. Herein, contribution of geogrid layers was considered and tensile strength values for model geogrid were given as discussed above in the slope stability analysis.

Figure 18 presents variation of factor of safety of a 4 m high geogrid reinforced coal ash embankment (with a blanket layer) with an applied footing pressure. As can be noted from Figure 18, immediately after subjecting the slope to a load equivalent to 300 kPa, the factor of safety has attained a value equal to 1. Majority of reinforcement layers in the upper half zone were found to be strained and ruptured.

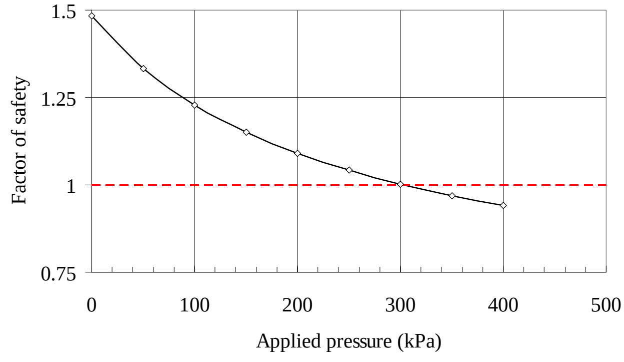

Figure 18 Variation of factor of safety with applied pressure for model REM14

This implies that there is a need for use of high strength geogrid reinforcement layers within in the geogrid reinforced slope is mandatory. This was found to be in agreement with the results published by Sommers and Viswanadham (2009). According to them, there is a need to strengthen the slope loaded externally loaded externally through a strip footing in the upper half to reduce straining and rupturing of reinforcement layers.

5. CONCLUSIONS

Based on the analysis and interpretation of centrifuge test results, the following conclusions can be drawn:

The above information obtained from centrifuge tests indicate that coal ash can be used for constructing rail embankments. Adequate measures shall have to be taken to provide drainage, provision of a side soil cover of thickness not less than 1.5 m and suitable berms for embankments of heights of the order of 11 m. In the case of geogrid reinforced coal ash embankment, geogrid layers were noticed to subject to strains higher than their respective ultimate strain values within top-half zone. This implies that there is a need for use of high strength geogrid reinforcement layers within in the geogrid reinforced embankments is mandatory.

Geogrid reinforcement layers in a reinforced coal ash embankment with 2V:1H slope were observed to experience straining after applying a bearing pressure of 250 kPa in the top-half zone and indicating a need to provide high strength layers in top-half zone. Further, results of stability analysis of soil confined coal ash embankment models constructed with coal ash as a fill material were found to corroborate well with physically observed centrifuge test results.

However, it will be interesting to construct in the field on pilot scale basis for evaluating the performance of rail embankments subjected to real loading and climatic conditions.

6. ACKNOWLEDGEMENTS

The authors would like to thank the Centrifuge team at the National Geotechnical Centrifuge Facility of Indian Institute of Technology Bombay, Powai, Mumbai-400076, India for their untiring support throughout the present study. Thanks are also due to M/s NTPC Limited, Noida, India for sponsoring the study.

7. REFERENCES

Chandrasekaran, V.S. (2001) “Numerical and centrifuge modelling in soil structure interaction”. Indian Geotechnical Journal, 31, Issue 1, pp 30–59.

Das, A., Jayashree, Ch.,Viswanadham, B.V.S. (2009) “Effect of randomly distributed geofibers on the piping behaviour of embankments constructed with fly ash as a fill material”. Geotextiles and Geomembranes, 27, Issue 5, pp 341-349.

Faber, J. H., and DiGioia Jr., A. M. (1976) “Use of fly ash in embankment construction”. Transportation Research Record, No. 593, pp 13-19.

Geostudio (2007) Geo-Slope, User's Manual for SEEP/W and SLOPE/W: Version 4, Geo-Studio International, Canada.

Gray, D. H., and Lin, Y. K. (1972) “Engineering properties of compacted fly ash,” J. Soil Mech. and Found. Div., ASCE, 98, Issue SM4, pp 361-380.

Leonards, G.A., Balley, B. (1982) “Pulverized coal ash as structural fill.” Journal of Geotechnical Engineering, ASCE, 108, Issue GT4, pp 517 - 531.

Lewis, T.S. (1976) “Construction of fly ash in roadway embankment in Illnois”. Transportation Research Record ,No. 593, pp 20-23.

Martin J. P., Collins, A. C., Browning, J.S., and Biehl, F.J. (1990) “Properties and use of fly ash for embankments”. Journal of Energy Engineering, ASCE, 116, Issue 2, pp 71-85.

NTPC report (2008) "Centrifuge model studies on the performance of rail embankments constructed with coal ash". Indian Institute of Technology Bombay, India.

Rajesh, S., and Viswanadham, B.V.S. (2012) "Modelling and instrumentation of geogrid reinforced soil barriers of landfill covers". Journal of Geotechnical and Geoenvironmental Engineering, ASCE, 138, Issue 1, pp 26-37.

Schofield, A. (1980) "Cambridge geotechnical centrifuge operations". Geotechnique, 30 , Issue 3, pp 227-268.

Sommers, A.N., and Viswanadham, B.V.S. (2009) "Centrifuge model tests on the behaviour of strip footings on geotextiles reinforced slopes". Geotextiles and Geomembranes, 27, Issue 6, pp 497-505.

Sunaga, M., and Sekine, E. (1992) "Utilization of fly ash as materials for railway embankment". Japanese Railway engineering, 121, October, pp. 13.

Sridharan., A., Pandian, N.S., and Prasad.P.S. (2000) "Liquid limit determination of class F fly ash". Journal of Testing and Evaluation, ASTM, 28 , Issue 6, pp 455-461.

Toth, P.S., Chan, H. T., and Cragg, C.B. (1988) "Coal ash as structural fill with reference to Ontario experience". Canadian Geotechnical Journal, 25, Issue 4, pp 694 - 704.

Viswanadham, B. V. S., and König, D. (2004) "Studies on scaling and instrumentation of a geogrid". Geotextiles and Geomembranes, 22, Issue 5, pp 307-328.

Viswanadham, B.V.S., Jha, B.K., and Sengupta, S.S. (2009) "Centrifuge testing of fiber reinforced soil liners for waste containment systems". Journal of Practice Periodical of Hazardous, Toxic, and Radioactive Waste Management, ASCE, 13, Issue1, pp 45-58.

Viswanadham, B. V. S., Das, A., and Mathur, V. K. (2012) "Centrifuge Model Tests on Rail Embankments Constructed with Coal Ash as a Structural Fill Material". Geo-Congress 2012, ASCE, Special Publication No. 225, Oakland, CA, USA, pp 3786-3795.